

A Desktop Multi-Material 3D Bio-Printing System with Open-Source Hardware and Software

Jaehoo Lee¹, Kyu Eon Kim¹, Sumi Bang³, Insup Noh^{2,3}, and Chibum Lee^{1,#}

¹ Department of Mechanical System & Design Engineering, Seoul National University of Science and Technology, 232 Gongneung-ro, Nowon-gu, Seoul, 01811, South Korea

² Department of Chemical & Biomolecular Engineering, Seoul National University of Science and Technology, 232 Gongneung-ro, Nowon-gu, Seoul, 01811, South Korea

³ Convergence Institute of Biomedical Engineering & Biomaterials, Seoul National University of Science and Technology, 232 Gongneung-ro, Nowon-gu, Seoul, 01811, South Korea

Corresponding Author / E-mail: chibum@seoultech.ac.kr, TEL: +82-2-970-6337, FAX: +82-2-974-8270

KEYWORDS: 3D printing, Multi-material bio-printing, 3D bio-printing system, Scaffold, Design of experiment, Open-source

Three-dimensional (3D) printing technology is considered to be a major driving innovation in tissue engineering, since a custom-made manufacturing for patients is essential for tissue and organ generation. Depending on the bio-materials and the applications, various 3D bio-printing technologies are used. A system capable of printing a variety of bio-materials through various methods is required for fabrication of hybrid scaffolds for tissue engineering research. This paper describes the design and integration of a multi-channel 3D bio-printing system at an affordable price based on open source hardware and software. The hardware and software components of the 3D bio-printing system and the process of finding optimal printing conditions are described in the paper. Fabrication of the hybrid scaffold of synthetic polymer and cell loaded hydrogel are presented to validate the performance of the system.

Manuscript received: September 7, 2016 / Revised: January 11, 2017 / Accepted: January 31, 2017

1. Introduction

Ever since the release of RepRap project as open source in 2005, rapid development of 3D printing technology was observed, along with increase in its market size and application areas.¹ 3D printing technology plays a major role in transferring mass production to small quantity batch production in manufacturing. 3D printing has been applied in various fields, such as automotive, medical, aviation, and architecture. Among these, tissue engineering can be considered as the most appropriate field for 3D printing technology. This is because custom-made manufacturing for patients is essential and its utilization is far superior. During organ transplantation, finding a suitable organ donor is very difficult, and even if found, several underlying problems remain leading to rejection of transplantation. To address such issues, a large volume of research is done on the fabrication of a variety of artificial organs or alternatives based on tissue engineering. In this regard, 3D bio-printing technology has secured an important position in this field.²⁻⁴

Fraunhofer Institute for Laser Technology in Germany developed an artificial blood vessel through a project called ArtiVasc 3D combining inkjet printing with stereolithography from 2011 to 2015.⁵ Organovo, regenerative medicine manufacturer in the United States has reached the commercialization stage with bio-printed liver tissue recently, and succeeded in bio-printing of artificial kidney tissue in 2016.⁶

In 3D bio-printing, along with the deposition of bio-materials, biochemical and living cells layer-by-layer, the placement of functional components is important.⁷ 3D bio-printing technology used in tissue engineering research varies depending on the target application and the properties of the bio-materials. Materials properties that are required for 3D bio-printing are ‘viscosity’ to determine the printability and the structure of output, ‘mechanical properties’ to maintain the desired shape inside the body, ‘biocompatibility’ which does not cause autoimmune reactions and is useful for cell activity and cell signaling, and ‘bio-degradability’ for supporting materials in which the scaffold is decomposed for necessary space where cells can be grown.⁷⁻¹¹

3D bio-printing technology is still in its initial stage. The main 3D bio-printing technology for deposition of bio-materials are ‘ink jet system’ that utilizes high temperature vaporization or piezoelectric effects,¹²⁻¹⁵ ‘micro-extrusion method’ that utilizes the pneumatic pressure or piston displacement,¹⁶⁻¹⁸ and ‘laser induced transfer’.¹⁹ ‘Fused deposition modeling’ by melting the thermoplastic biopolymer filament,²⁰ and ‘stereo-lithography’ by polymerizing photo curable materials have also been used.²¹ 3D bio-printed output primarily depends on what material and which method are the most compatible with actual tissues and organs, and to support this, equipment with a variety of materials and printing methods is required.

Most 3D bio-printing systems used in the on-going research or the

commercialized ones have a limit on the printing method provided, and the materials that can be printed.²⁰⁻²² In addition, the price of 3D bio-printers with multi-axis configuration is high and becomes a barrier to bio research.^{6,23}

In the present study, we aimed to develop a low cost 3D bio-printing system with pneumatic and piston extrusion and need valve jet methods. The 3D bio-printing system should be able to accept a variety of bio-materials to build composite hybrid scaffolds for tissue engineering research. The hardware was designed by applying rotary mechanism for multi-channel printing and open architecture to accept any printing method. To reduce the cost, open source hardware and firmware were fully utilized which can be easily accessible to the 3D printing community.

The remainder of the paper is organized as follows. Section 2 provides a description of the 3D bio-printing system based on the open source hardware and software. In Section 3, the design of experiments (DOE) is described to find the optimal printing conditions for PLGA and hybrid hydrogels. Fabrications of 3D biostructures with single and composite materials validate the performance of the developed system in Section 4. Some observations and conclusions are presented in Section 5.

2. Development of 3D Bio-Printing System

A 3D bio-printing system was developed for 3D fabrication of composite structures of biological materials such as polymers or decellularized ECM (extracellular matrix) for scaffolds and cell loaded hydrogels, which are generally studied in tissue engineering. It is capable of printing various bio-materials in several dispensing methods. This multi-channel 3D bio-printing system was built with inexpensive linear stages and a rotary table to achieve a low-cost, small-sized, and expendable system. Compared to the system produced by EnvisionTEC and RegenHU, the cost of multi-material 3D Bio-printing system developed in this study has been reduced more than 1/10 times and the number of allowable channels and the expandability of diverse printing methods are similar level.²⁴

2.1 Requirement for 3D bio-printing system

To prevent contamination and maintain a stable environment in manufacturing process, the 3D bio-printing system was designed so that it can be used on a small-sized clean bench of dimension 920 mm × 600 mm × 600 mm (W × D × H).

The 3D bio-printing system can print various bio-materials including hydrogels with various viscosity, thermoplastic biodegradable polymers, and ceramics. To expand the use of the 3D bio-printing system to another material and dispensing method in the future, a multi-channel replaceable dispensing system is required.

2.2 Description of 3D bio-printing system

The 3D bio-printing system consists of positioning stages, bio-material dispensers and control system. By utilizing open-source hardware and software for 3D bio-printing system, expenditure becomes lower than the commercialized one and an open architecture for various printing method can be achieved. The schematics of 3D bio-printing

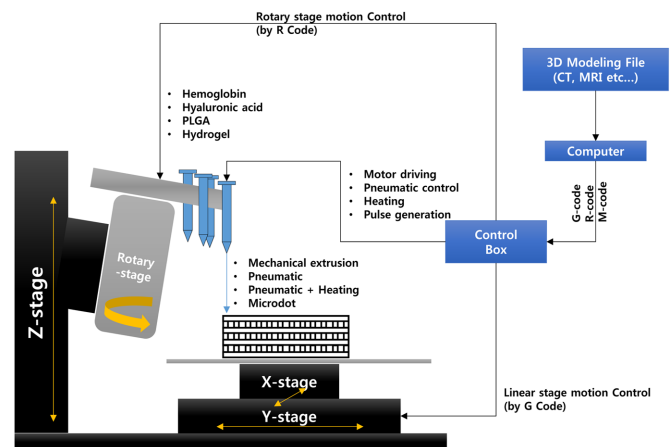


Fig. 1 Schematics of 3D bio-printing system

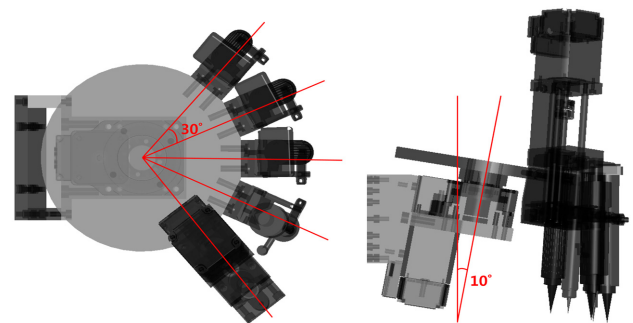


Fig. 2 Carousel multi-channel dispensing system

system is shown in Fig. 1.

2.2.1 Positioning stages

The positioning system was configured along X, Y, Z axes using 3 ball screw linear stages (SMI-0810-3S, Science Town Inc., Korea), which has bi-repeatability of $\pm 1.5 \mu\text{m}$ and is suitable for printing objects with a stroke of 100 mm. Each stage can be controlled by the stepper motor (Ezi-SERVO-MI-42M-A, Fastech co., Korea).

The 3D bio-printing system adopted the carousel dispensing system²⁵ with a rotary actuator (HG60, Fastech co, Korea) in order to realize multi-channel dispensing in limited space as shown in Fig. 2. The rotary actuator which has repetitive positioning accuracy of ± 0.0028 degree and was operated by a stepper motor was mounted with a tilting angle of 10 degrees from the vertical axis to prevent impingement of inactive channel and secure spare space in the bottom of the dispensers. Two grooved ball bearing in the rotary actuator maximized allowable axial loads and moment load, while the structural analysis confirmed sufficient allowable load which was much higher than attaching 1 mechanical extruder, 3 pneumatic extruders and 1 needle valve jet in tilted angle.

2.2.2 Dispensers for multi-material printing

The system designed for tissue engineering research comprised the pneumatic and mechanical extrusion for continuous dispensing and needle valve inkjet for drop-on-demand dispensing in order to accommodate a range of possible properties with each material. The

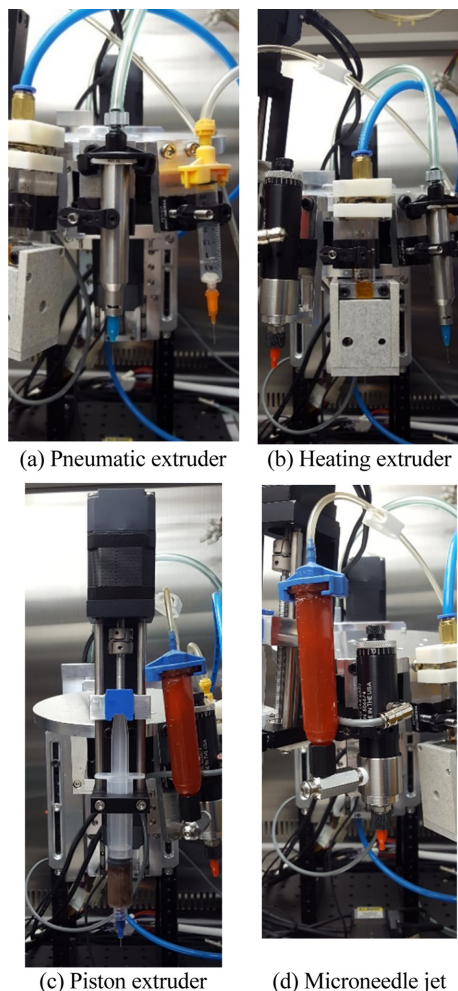


Fig. 3 Various types of dispensers

dispensing system was designed so that depending upon the bio-material and the component of the hybrid scaffold, the exchangeable dispensers could be selected and attached to the rotary actuator.

The pressure of pneumatic extrusion in Fig. 3(a) is controlled up to 900 kPa using the electro-pneumatic regulator (ITV2050, SMC Co., Japan). The oil-free compressor (BEETLE BUG, YAMATO Co., Japan) supplies the pneumatic pressure, and the air cleaning filter (SFD100-02B, SMC Co., Japan) prevents contamination and damage of the electro-pneumatic regulator. To melt and dispense the thermoplastic biopolymer, such as PLGA or PCL, an in-house machined heating block with a ceramic heater and a K-type thermocouple sensor is attached to one pneumatic extruder in Fig. 3(b).

As shown in Fig. 3(c), a small size, low weight mechanical extruder was developed considering the load on the rotary actuator. The mechanical extruder was designed based on the open source syringe pumps²⁶ and consisted of stepper motor (EzM-42, Fastech Co., Korea), ball screw (LMKR0601KS-C7K-130R130, LM Korea, Korea) with 1 mm lead, and ball bearing. The mechanical extrusion showed the advantage of accurate dispensing, and thus, was used for dispensing high viscous bio-materials, such as ceramic or TCP (Tri Calcium Phosphate), which the pneumatic extruder cannot dispense accurately.

Furthermore, in order to print a high-molecular hydrogels containing

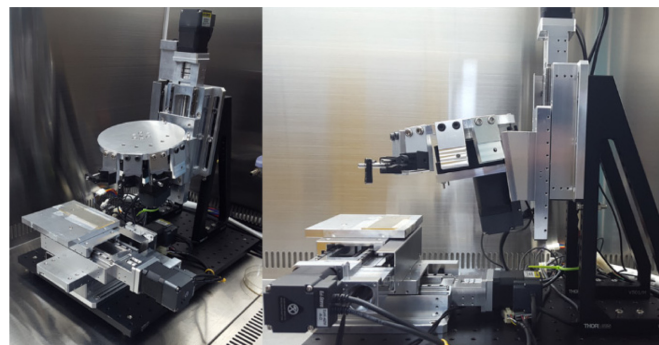


Fig. 4 Multi-channel 3D bio-printing system

tiny amount of cells, the pneumatic micro needle valve (741MD, Nordson EFD, USA) in Fig. 3(d) and a valve controller (ValveMate7100, Nordson EFD, USA) were adopted for drop-on-demand dispensing. With such a system, it was possible to adjust the size of the droplets of high viscous hydrogels containing cells, in other words, the number of cells can be controlled approximately.

2.2.3 Control system

A control unit for the 3D bio-printing system was built with the open source hardware, Arduino. Arduino Mega 2560 has 16 MHz microcontroller, 54 digital input and output pins, 16 analog inputs and 2 serial ports and has been used widely in open source 3D printers. An LCD display and user input buttons (Smart LCD Controller, Reprapdiscount, USA) were implemented for the user's convenience and standalone operation. The hardware control is based on the open-source firmware Marlin²⁷ which is widely used in Arduino based 3D printers. Marlin was developed for FDM (Fused Deposition Modeling) 3D printers by many professional contributors and has many advanced features, including arc motion, look ahead algorithms and etc.

In the present study, Marlin was modified to make it suitable for the developed 3D bio-printing system. The operation of the printing system was based on G codes which are the most widely used numerical control programming language and used in most 3D printers. In addition, R codes for carousel multi-channel dispensing system, E codes for mechanical extrusion, and M codes for pneumatic extrusion and needle valve inkjet were newly defined or modified in the firmware.

The stepper motors (EzS-PD-42, Fastech co., Korea) used in this system differ from general stepper motors, and has the integrated encoders and high performance DSP so that the internal feedback control can guarantee accurate positioning and achieve smooth motion without ripples.

The independent temperature controller (Extruder controller 2, Seedstudio Co., China) adjusts the current to the ceramic cartridge heater with PID (Proportional-Integral-Derivative) control to regulate the temperature of aluminum block. Typically, the set point for temperature control is chosen between glass transition and melting temperatures of thermoplastic biopolymers to obtain the best printing performance.

The developed 3D bio-printing system was located inside a clean bench as shown in Fig. 4. It comprised 1 piston extruder, 1 needle valve jet, 2 pneumatic extruders and 1 pneumatic extruder with heat block.

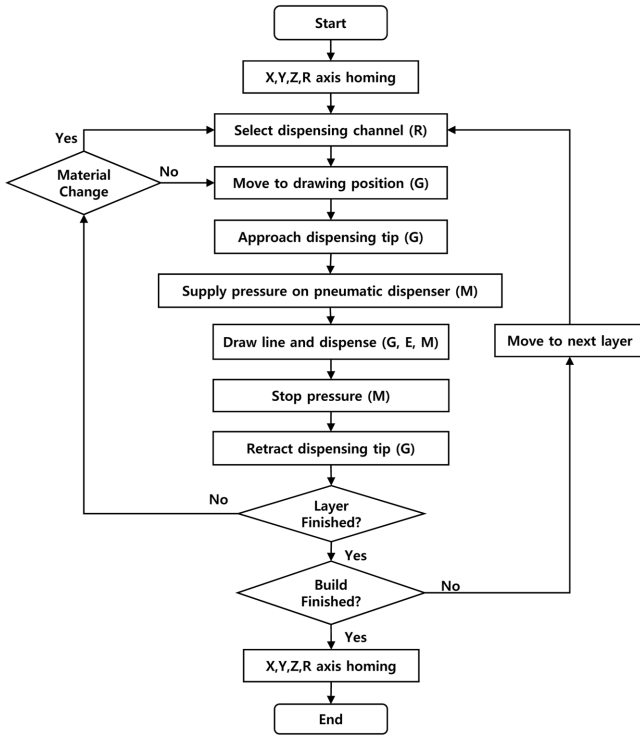


Fig. 5 Control flowchart

The maximum build size is 100 mm × 100 mm × 100 mm and the positioning accuracy is 0.001 mm.

The positions of dispensing nozzles varied after installation of dispensers. Thus calibration process were required before printing. After installation, small amount of each materials was dispensed by rotating the carousel. The deviated position compared to the first nozzle was measured and were used in an in-house built software to compensate the position distance. To use the 3D bio-printing system, 3D CAD models designed to fit the individual characteristics, were converted to G-codes by 3D printing slicing software such as an open source software Cura.²⁸ Next, the code was modified to add M code, R code, and E code using the in-house built software. This code governed the operation of the positioning stages including rotary actuator, the mechanical and pneumatic dispensers and the needle valve inkjet to compensate the variation of the dispenser position. The firmware in the micro-controller ran the modified code. A flow chart for modified firmware is shown in Fig. 5.

3. Experimental Design for Bio-Printing

To perform the 3D printing by different methods for different materials, the optimum printing conditions with respect to each material needs to be found. In this section, the optimum printing conditions for PLGA and hydrogel has been described through single line test.

The optimum printing conditions for PLGA and hydrogels were determined using the Box-Behnken experimental design combined with response surface modeling and quadratic programming. The Box-Behnken designs are generally applied where the number of experiments is small, but the first and second order coefficient can be estimated efficiently.²⁹

Table 1 Design matrix for PLGA printing condition

Order	Pressure [kPa] (<i>P</i>)	Feed rate [mm/min] (<i>F</i>)	Layer thickness [mm] (<i>z</i>)	Line width [μm] (<i>w</i>)
1	220	250	0.20	185.0
2	220	200	0.20	208.8
3	250	250	0.25	216.8
4	250	225	0.20	220.8
5	250	250	0.15	218.8
6	220	225	0.15	199.3
7	250	200	0.25	210.6
8	280	225	0.15	269.2
9	250	225	0.20	204.0
10	280	250	0.20	220.0
11	280	200	0.20	233.3
12	250	200	0.15	225.9
13	280	225	0.25	198.4
14	220	225	0.25	168.5
15	250	225	0.20	200.2

3.1 Optimum condition for printing PLGA

Typically, the scaffold is made of biocompatible and biodegradable materials that can be so absorbed in the body after a certain period. Among several biodegradable polymers, poly (lactic-co-glycolide) (PLGA) (lactide:glycolide 75:25, Sigma-Aldrich, USA) was chosen as a scaffold. Biopolymers of PLGA has been used widely for 3 dimensional scaffold fabrication, because of certain advantages, such as control of the degradation rate by controlling the molar ratio of Lactic and Glycolic acids, stable structure, and high mechanical strength.^{30,31}

The factors that influence melting and dispensing PLGA, are the heating temperature *T*, needle size *D*, feed rate of the XY stage *F*, applied pneumatic pressure *P*, and *z* layer thickness *z*. Among these factors, the heating temperature *T*, the needle size *D* were fixed at 130°C, and 27G (ID 200 μm), respectively, while the other factors were chosen as design variables. The line width *w* was chosen as 200 μm for optimum output, because it can provide sufficient mechanical strength and proper porosity. Based on the typical Box-Behnken matrix of 3 factors, a total of 15 experiments (see Table 1) were done out of which 13 experiments corresponded to the range of conditions for each level of each factor, and 2 overlapping experiments were for improving reliability.

The 3D response surface diagrams between 2 independent variables and line width are shown in Fig. 6. Multiple regression on the design matrix gave the quadratic response surface equation

$$\begin{aligned}
 w = & 493.278 + 2.80585P - 6.13747F + 229.205z \\
 & + 0.0035PF - 6.67083Pz + 2.657Fz - 0.00319P^2 \\
 & + 0.01009F^2 + 1358.13z^2
 \end{aligned} \quad (1)$$

From the results of the response surface regression, the value of R-sq (explanatory power of regression), 79.55%, and lack of fit value 0.23 confirmed the reliability of explanatory power of regression equation and suitability of the model.

The optimum condition for printing line width of 200 μm was obtained using pressure *P* of 220 kPa, feed rate *F* of 200 mm/min, and layer height *z* of 195.5 μm. The validation experiment under the above-mentioned conditions generated line width with an average of 204 μm, which was accurate enough with 2% error as shown in Fig. 7(a).

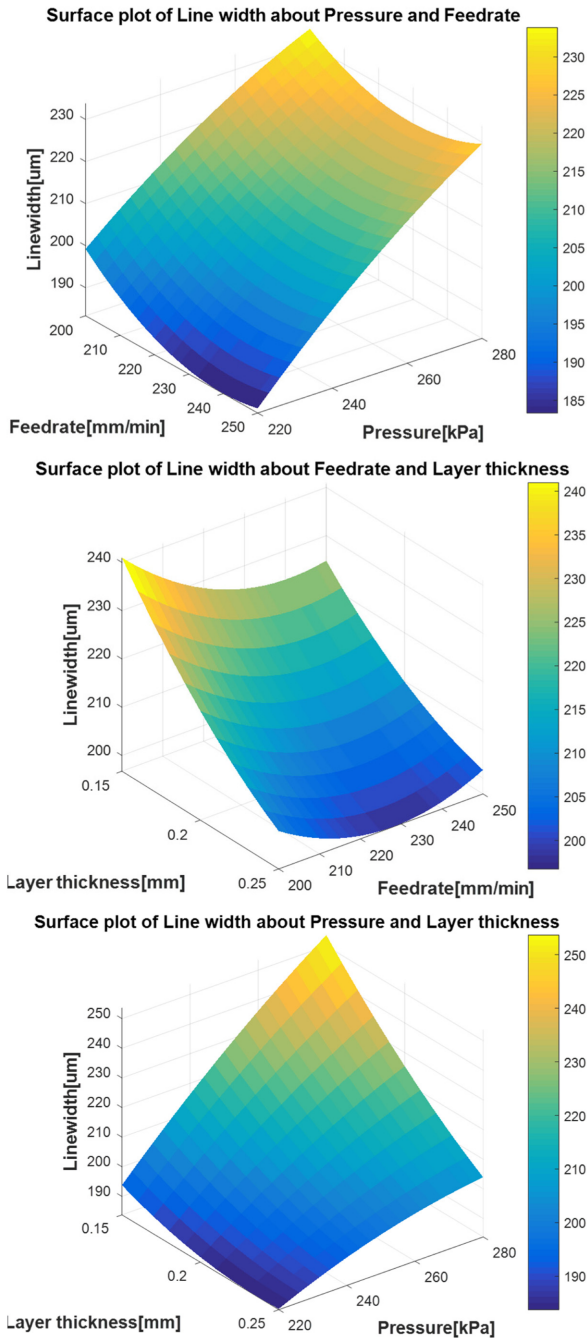


Fig. 6 3D response surface diagrams for PLGA line width

However, the starting and ending parts of the line have non-uniform width when pneumatic extrusion is used. Approximately 700 μm from start and end positions shows non-uniform width almost 2 times in the start and stop position. Further research will be required to get the constant line width in starting and ending parts.

3.2 Optimum condition for printing hydrogels

The polymeric hydrogels used in this study was obtained through a Michael type addition reaction between hyaluronic acid-tri(carboxyethyl) phosphine (HA-TCEP) and hyaluronic acid-acrylate (HA-AC). The experimental done for the hydrogel was similar to that for PLGA.

The printing of the hydrogel depends on the concentration of the

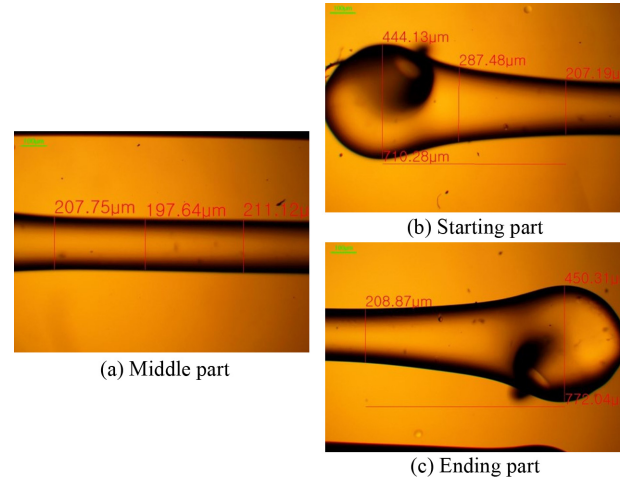


Fig. 7 Validation experimental results

Table 2 Design matrix for hydrogel printing condition

Order	Gelation time [min] (t)	Pressure [kPa] (P)	Feed rate [mm/min] (F)	Line width [μm] (w)
1	9	320	350	480.2
2	9	380	350	592.3
3	7	350	420	1019.5
4	8	380	280	1020.7
5	8	320	280	888.0
6	8	320	420	756.1
7	8	380	420	809.4
8	7	380	350	1447.5
9	8	350	350	908.5
10	8	350	350	856.6
11	9	350	420	607.4
12	7	320	350	809.8
13	8	350	350	927.9
14	9	350	280	612.3
15	7	350	280	1059.1

hyaluronic acid C , the gelation time after mixing t , needle size D , feed rate of the XY stage F , applied pneumatic pressure P , and layer thickness z . Among these factors, the concentration of hyaluronic acid C was fixed at 5%, the needle size D at 23G (ID 400 μm), the layer thickness in Z direction z at 0.3 mm. After mixing the hyaluronic acid, the solution started gelation rapidly and viscosity depended on the time after mixing. z layer height z which was weekly affecting variable for hydrogel is excluded from design variables.

Box-Behnken design matrix is given in Table 2 and response surface is given by

$$w = -166581.1 + 2107.7t + 50.5081P + 4.26685F - 438tP + 0.12393tF - 0.00945PF + 54.5958t^2 - 0.0118P^2 - 0.00377F^2 \quad (2)$$

From the response surface, the optimum conditions derived for printing Hydrogel line width of 400 μm were as follows: gelation time after mixing t was 9 minutes, feed rate F was 287 mm/min, and pressure P was 327 kPa. The experiment when done under the optimum conditions generated line width with 9% error.

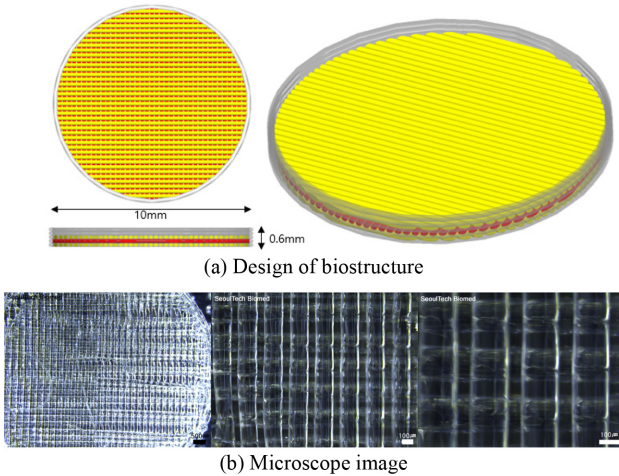


Fig. 8 PLGA cylinder with lattice structure

4. Fabrication of Hybrid Scaffold with 3D Bio-Printing System

Based on the optimal conditions derived for PLGA and hydrogel, various 3D biostructures with multi-materials as well as single materials were fabricated.

4.1 Fabrication of scaffold with single material

4.1.1 PLGA cylinder with lattice structure

The PLGA cylinder with inside lattice, which would be used as scaffold for cell laden hydrogel in future research, was fabricated. PLGA was melted at 130°C and the printing condition obtained in section 3.1 was used. The cylinder was fabricated with line width of 0.2 mm and the inner lattice formed pores of 0.05 mm × 0.05 mm. The diameter of the cylinder was 10 mm and the height was 0.6 mm as shown in Fig. 8.

4.1.2 Hydrogel lattice

In order to fabricate a scaffold only with the hydrogel, the hydrogel made from 5% (w/v) hyaluronic acid was printed under the obtained optimum conditions to form pores of 0.6 mm × 0.6 mm with line width of 0.4 mm and stacked up to a height of 1.6 mm. As shown in Fig. 9, the structure was not accurate enough to form the intended design, but it can be used for scaffold-free tissue fabrication study later.

4.1.3 α-TCP lattice

Beside PLGA and hydrogel, many possible biomaterials can be used in 3D bio-printing. α-TCP is a bio-absorbable ceramic used in the production of medical products such as calcium fortifier or artificial bones. A lattice scaffold with α-TCP (Tricalcium Phosphate) was also tried. Printing α-TCP is challenging because there are strong interactions between the particles and it solidifies easily after mixing with hydrogel. Thus, the pneumatic extrusion could not dispense consistently and the mechanical extrusion was used. Mechanical extrusion can regulate the output by controlling the piston displacement.

The structure was composed of 16 lines inside 15 mm × 15 mm in each layer and stacked up to 0.8 mm along with 225 pores of size 0.85 mm × 0.85 mm.

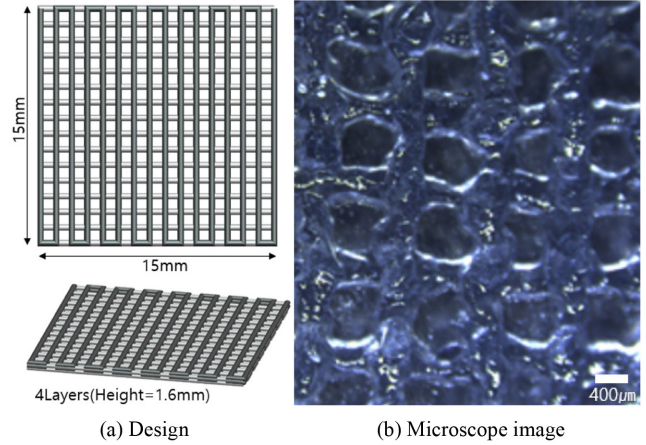


Fig. 9 Hydrogel lattice scaffold

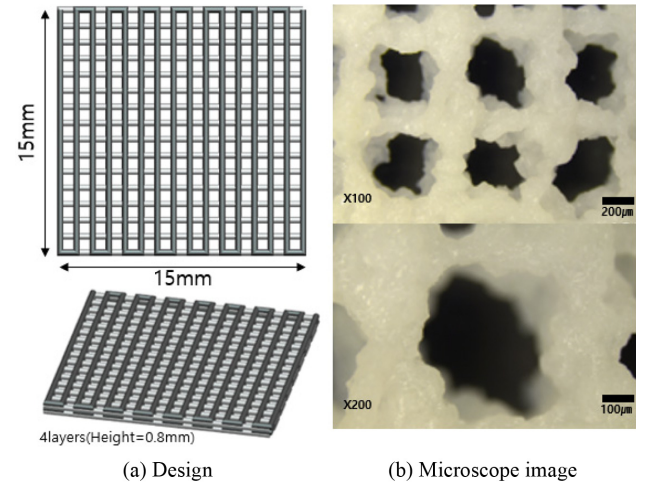


Fig. 10 Microscope image of lattice scaffold manufactured by α-TCP

When the layer height is equal to the nozzle diameter, the deposition velocity Eq. (3) can be analytically calculated from the nozzle diameter D , and flow rate Q ³²

$$F_N = \frac{4Q}{\pi D^2} \quad (3)$$

The printing conditions were as follows: extrusion rate Q of 1 mL/min, feed rate F of 100 mm/min, and layer height z of 200 µm. The printed structure is shown in Fig. 10. Even though each layer was not stacked up clearly, but we can still build the intended shape roughly.

4.2 Fabrication of hybrid scaffold

To not limit the usage of the developed bio-printing system to a single material, 3D hybrid scaffolds were fabricated with composite bio-materials.

4.2.1 Scaffold of 2 hydrogels

To investigate the interaction of different hydrogels, the other type of hydrogel was printed in line between the lattices of the hydrogels containing hyaluronic acid.

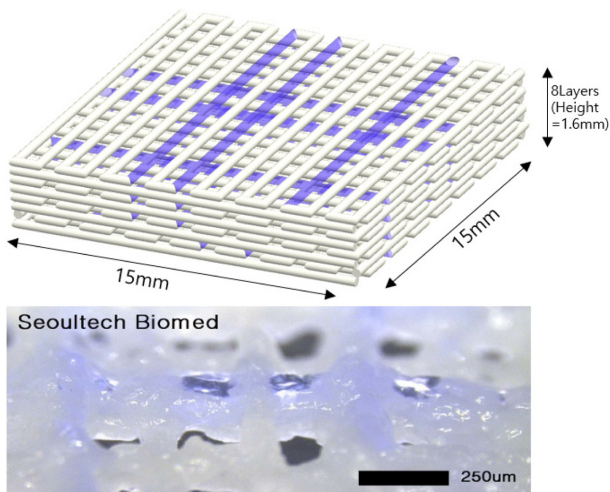


Fig. 11 Lattice scaffold with 2 hydrogels

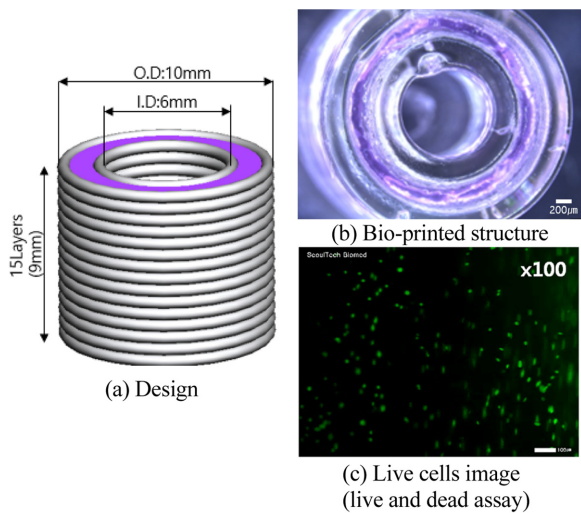


Fig. 12 Cylinder hybrid scaffold with PLGA and hydrogels

Pneumatic extrusion was used for printing two hydrogels under different conditions. The structural design is shown in Fig. 11. Hydrogel 1 (5% hyaluronic acid and α -TCP (tricalcium phosphate, v/v ratio, 30:1)) was used as base scaffold and printed under the conditions mentioned in section 3.2. The printing conditions of hydrogel 2 (5% Hyaluronic acid hydrogel) also determined through experiment, are: gelation time 6 minutes, feed rate 180 mm/min and applied pneumatic pressure 300 kPa.

4.2.2 3D cylinder scaffold of PLGA and cell laden hydrogel

Fig. 12 shows the PLGA double-walled cylindrical scaffold containing the cell laden hydrogel inside. A double-walled cylinder with outer diameter 10 mm, inner diameter 6 mm and height 9 mm was fabricated under the conditions obtained in section 3. The diameters of the inner and the outer cylinders were 9 mm, and 10 mm, respectively. The hyaluronic hydrogel containing human fibroblast were filled up between the outer and inner walls under the following conditions: applied pressure 200 kPa, feed rate 300 mm/min and nozzle diameter 250 μ m. This

hybrid scaffold is the preliminary fabrication of bone blood vessel research. Due to opaqueness of the thick gel, we could not observe cells deep inside but no dead cells were found as Fig. 12(c). This hybrid scaffold is the preliminary fabrication of bone blood vessel research.

5. Conclusions

The availability of compact, multi-channel bio-printing system will expedite the technology of 3D bio-printing and contributes the development of the biomedical and tissue engineering research. The affordable but versatile 3D bio-printing system with multi-channel and open architecture platform is required to further develop the biomaterial science, cell biology, medicine and associated applications for 3D bio-printing researchers.

A compact, multi-channel 3D bio-printing system was developed at affordable price based on open source hardware and software. The 3D bio-printing system adopted rotary mechanism for multi-channel printing and open architecture to accept any printing method. The hardware and software components which were inspired by open-source and their integration were described. Experimental design was carried out to obtain optimal printing conditions with single line test. Several hybrid scaffolds with synthetic polymer and cell laden hydrogels were fabricated and the performance of the developed 3D bio-printing system was verified. Currently, cell culture of the printed hybrid scaffold is under progress. Based on the optimal conditions for PLGA and hydrogel, various 3D biostructures containing multi-materials as well as single materials were fabricated.

ACKNOWLEDGEMENT

This work was supported by the National Research Foundation of Korea (NRF) Grant (2015R1A2A1A10054592 and 2014K2A2A7060 928) and the MOTIE (Ministry of Trade, Industry & Energy) and the KIAT (Korea Institute for Advancement of Technology) through the Industry Convergence/Connected for Creative Robot Human Resource Development (N0001126).

REFERENCES

1. Lipson, H. and Kurman, M., "Fabricated: The New World of 3D Printing," John Wiley & Sons, pp. 1-5, 2013.
2. Ozbolat, I. T. and Yu, Y., "Bioprinting Toward Organ Fabrication: Challenges and Future Trends," IEEE Transactions on Biomedical Engineering, Vol. 60, No. 3, pp. 691-699, 2013.
3. Varkey, M. and Atala, A., "Organ Bioprinting: A Closer Look at Ethics and Policies," Wake Forest JL & Pol'y, Vol. 5, pp. 275-298, 2015.
4. Mironov, V., Kasyanov, V., Drake, C., and Markwald, R. R., "Organ Printing: Promises and Challenges," Regenerative Medicine, Vol. 3, No. 1, pp. 93-103, 2008.

5. Fraunhofer, Ltd., "ArtiVasc 3D," <http://www.artivasc.eu/en/projectdetails.html> (Accessed 20 MAR 2017)
6. Organovo, "ExVive™ Human Tissue Models & Services for Research," <http://organovo.com/tissues-services/exvive3d-human-tissue-models-services-research/> (Accessed 20 MAR 2017)
7. Murphy, S. V. and Atala, A., "3D Bioprinting of Tissues and Organs," *Nature Biotechnology*, Vol. 32, No. 8, pp. 773-785, 2014.
8. Malda, J., Visser, J., Melchels, F. P., Jüngst, T., Hennink, W. E., et al., "25th Anniversary Article: Engineering Hydrogels for Biofabrication," *Advanced Materials*, Vol. 25, No. 36, pp. 5011-5028, 2013.
9. Peltola, S. M., Melchels, F. P. W., Grijpma, D. W., and Kellomäki, M., "A Review of Rapid Prototyping Techniques for Tissue Engineering Purposes," *Annals of Medicine*, Vol. 40, No. 4, pp. 268-280, 2008.
10. Bose, S., Roy, M., and Bandyopadhyay, A., "Recent Advances in Bone Tissue Engineering Scaffolds," *Trends in Biotechnology*, Vol. 30, No. 10, pp. 546-554, 2012.
11. Williams, D. F., "On the Mechanisms of Biocompatibility," *Biomaterials*, Vol. 29, No. 20, pp. 2941-2953, 2008.
12. Klebe, R. J., "Cytoscribing: A Method for Micropositioning Cells and the Construction of Two-And Three-Dimensional Synthetic Tissues," *Experimental Cell Research*, Vol. 179, No. 2, pp. 362-373, 1988.
13. Xu, T., Zhao, W., Zhu, J.-M., Albanna, M. Z., Yoo, J. J., and Atala, A., "Complex Heterogeneous Tissue Constructs Containing Multiple Cell Types Prepared by Inkjet Printing Technology," *Biomaterials*, Vol. 34, No. 1, pp. 130-139, 2013.
14. Xu, T., Jin, J., Gregory, C., Hickman, J. J., and Boland, T., "Inkjet Printing of Viable Mammalian Cells," *Biomaterials*, Vol. 26, No. 1, pp. 93-99, 2005.
15. Cui, X., Boland, T., D D'Lima, D., and K Lotz, M., "Thermal Inkjet Printing in Tissue Engineering and Regenerative Medicine," *Recent Patents on Drug Delivery & Formulation*, Vol. 6, No. 2, pp. 149-155, 2012.
16. Cohen, D. L., Malone, E., Lipson, H., and Bonassar, L. J., "Direct Freeform Fabrication of Seeded Hydrogels in Arbitrary Geometries," *Tissue Engineering*, Vol. 12, No. 5, pp. 1325-1335, 2006.
17. Iwami, K., Noda, T., Ishida, K., Morishima, K., Nakamura, M., and Umeda, N., "Bio Rapid Prototyping by Extruding/Aspirating/Refilling Thermoreversible Hydrogel," *Biofabrication*, Vol. 2, No. 1, Paper No. 014108, 2010.
18. Shor, L., Güçeri, S., Chang, R., Gordon, J., Kang, Q., et al., "Precision Extruding Deposition (PED) Fabrication of Polycaprolactone (PCL) Scaffolds for Bone Tissue Engineering," *Biofabrication*, Vol. 1, No. 1, Paper No. 015003, 2009.
19. Barron, J. A., Wu, P., Ladouceur, H. D., and Ringeisen, B. R., "Biological Laser Printing: A Novel Technique for Creating Heterogeneous 3-Dimensional Cell Patterns," *Biomedical Microdevices*, Vol. 6, No. 2, pp. 139-147, 2004.
20. Zein, I., Huttmacher, D. W., Tan, K. C., and Teoh, S. H., "Fused Deposition Modeling of Novel Scaffold Architectures for Tissue Engineering Applications," *Biomaterials*, Vol. 23, No. 4, pp. 1169-1185, 2002.
21. Kwon, I. K. and Matsuda, T., "Photo-Polymerized Microarchitectural Constructs Prepared by Microstereolithography (MSL) Using Liquid Acrylate-End-Capped Trimethylene Carbonate-Based Prepolymers," *Biomaterials*, Vol. 26, No. 14, pp. 1675-1684, 2005.
22. Norotte, C., Marga, F. S., Niklason, L. E., and Forgacs, G., "Scaffold-Free Vascular Tissue Engineering Using Bioprinting," *Biomaterials*, Vol. 30, No. 30, pp. 5910-5917, 2009.
23. Shim, J.-H., Lee, J.-S., Kim, J. Y., and Cho, D.-W., "Bioprinting of a Mechanically Enhanced Three-Dimensional Dual Cell-Laden Construct for Osteochondral Tissue Engineering Using a Multi-Head Tissue/Organ Building System," *Journal of Micromechanics and Microengineering*, Vol. 22, No. 8, Paper No. 085014, 2012.
24. 3D Printing Industry, "The Top 15 Bioprinters," <https://3dprintingindustry.com/news/top-10-bioprinters-55699/> (Accessed 20 MAR 2017)
25. Sutanto, E., Shigeta, K., Kim, Y., Graf, P., Hoelzle, D., et al., "A Multimaterial Electrohydrodynamic Jet (E-Jet) Printing System," *Journal of Micromechanics and Microengineering*, Vol. 22, No. 4, Paper No. 045008, 2012.
26. Wijnen, B., Hunt, E. J., Anzalone, G. C., and Pearce, J. M., "Open-Source Syringe Pump Library," *PLoS One*, Vol. 9, No. 9, Paper No. e107216, 2014.
27. RepRapWiki, "Marlin. Cura 3D Printing Slicing Software," http://reprap.org/wiki/Marlin_Cura_3D_Printing_Slicing_Software (Accessed 20 MAR 2017)
28. Ultimaker, "Cura Software," <https://ultimaker.com/en/products/cura-software> (Accessed 20 MAR 2017)
29. Box, G. E. P. and Behnken, D. W., "Some New Three Level Designs for the Study of Quantitative Variables," *Technometrics*, Vol. 2, No. 4, pp. 455-475, 1960.
30. Baker, S. C., Rohman, G., Southgate, J., and Cameron, N. R., "The Relationship between the Mechanical Properties and Cell Behaviour on PLGA and PCL Scaffolds for Bladder Tissue Engineering," *Biomaterials*, Vol. 30, No. 7, pp. 1321-1328, 2009.
31. Blanco, M. D., Sastre, R. L., Teijón, C., Olmo, R., and Teijón, J. M., "Degradation Behaviour of Microspheres Prepared by Spray-Drying Poly (D, L-Lactide) and Poly (D, L-Lactide-Co-Glycolide) Polymers," *International Journal of Pharmaceutics*, Vol. 326, No. 1, pp. 139-147, 2006.
32. Khalil, S. and Sun, W., "Biopolymer Deposition for Freeform Fabrication of Hydrogel Tissue Constructs," *Materials Science and Engineering: C*, Vol. 27, No. 3, pp. 469-478, 2007.